PAPER • **OPEN ACCESS**

Electron thermal conductivity of nickel and aluminum in solid and liquid phases in two-temperature states

To cite this article: Yu V Petrov *et al* 2021 *J. Phys.: Conf. Ser.* **1787** 012025

Electron thermal conductivity of nickel and aluminum in solid and liquid phases in two-temperature states

Yu V Petrov[1,2], N A Inogamov[1,3], V A Khokhlov[1] and K P Migdal[3]
[1] Landau Institute for Theoretical Physics of the Russian Academy of Sciences, Akademika Semenova 1a, Chernogolovka, Moscow Region 142432, Russia
[2] Moscow Institute of Physics and Technology, Institutskiy Pereulok 9, Dolgoprudny, Moscow Region 141701, Russia
[3] Dukhov Research Institute of Automatics (VNIIA), Sushchevskaya 22, Moscow 127055, Russia

E-mail: nailinogamov@gmail.com

Abstract. Analytical expressions for the electron thermal conductivity of nickel and aluminum are presented. The thermal conductivity depends on the electronic and ionic temperatures, density and phase of the substance (solid or liquid). The expressions obtained can be used in hydrodynamic calculations of the ablation of these metals or multilayer targets made from them. We consider the case when ablation is caused by the action of ultrashort laser pulses.

1. Introduction

When simulating ablation processes under the action of ultrashort laser pulses, hydrodynamic codes describing the motion of ablating matter are powerful instruments of investigations [1–3]. The hydrodynamic description is used when considering wide-gap dielectrics [4, 5], semiconductors [6, 7], metals [8–13]. Hydrodynamic modeling in particular is useful to study the damage of multilayer targets under the laser exposure. The essential component of the hydrodynamic equations describing the evolution of laser irradiated matter are kinetic coefficients, among which the electron thermal conductivity is very important, regulating the heat transfer from the initially heated region deep into the target. We study the ablation of multilayer target consisting of the alternating layers of nickel and aluminum under the ultrashort laser irradiation. In this connection it is important to have knowledge of the electron thermal conductivity of these metals in the two-temperature states with unequal electron and ion temperatures and varying density and phase state.

2. Electronic thermal conductivity of nickel in solid phase

In a number of works, we have performed the calculation of kinetic coefficients for metals widely used in physical experiments and technical applications, such as copper [14–17], gold [18–21], silver [22] and others [23]. Similar to how this was done for these metals, we write analytical expressions for the coefficient of electronic thermal conductivity of nickel and aluminum in two-temperature states with different electron and ion temperatures. These expressions should be

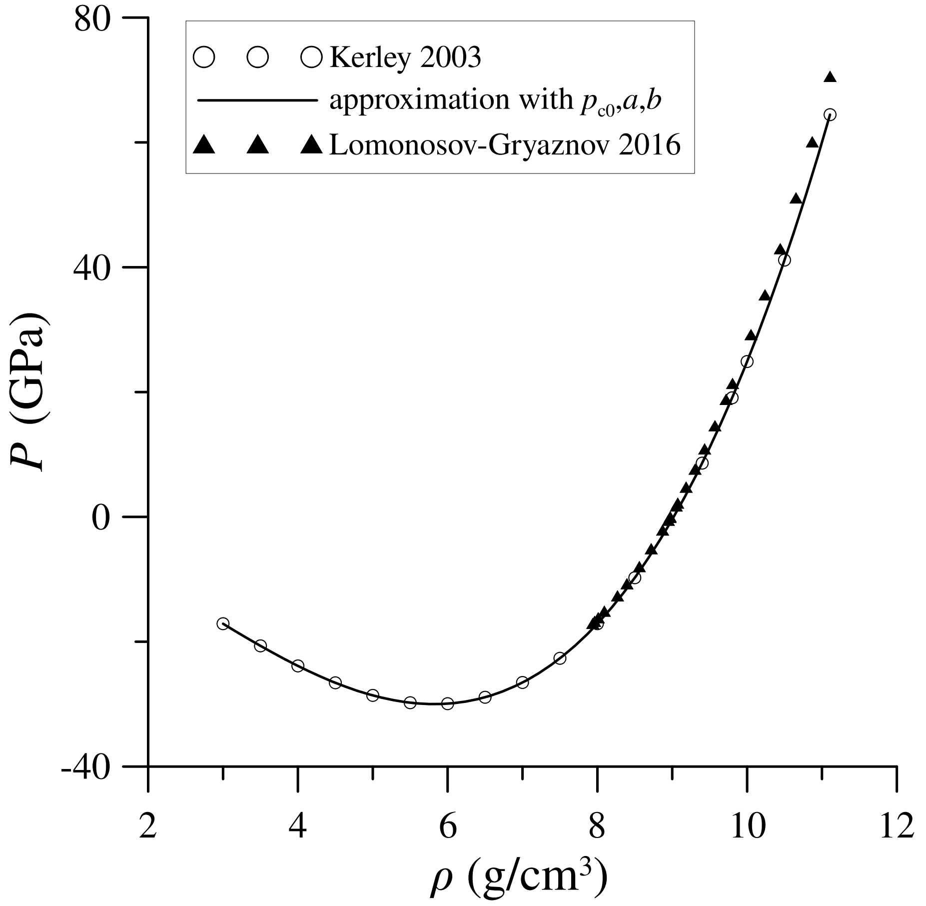

Figure 1. Cold pressure curve of nickel from the works [25, 26] and its approximation by the formula (7) (full line).

transferred to the more familiar single-temperature ones, since the hydrodynamic code used by us end-to-end describes the transition from the two-temperature stage with hot electrons in solid and liquid phases to the one-temperature stage.

Taking into account the thermal conductivity of s-electrons due to electron–ion and electron–electron collisions, the expression for the inverse coefficient of electron thermal conductivity κ_s (thermal resistance S_e) in the solid phase has the form

$$\frac{1}{\kappa_{\rm s}} = \frac{1}{\kappa_{\rm ee}} + \frac{1}{\kappa_{\rm ei}^{\rm s}} \tag{1}$$

in complete analogy with the well-known Matthiessen's rule for electrical conductivity [24], due to the addition of the scattering probabilities per unit time for these two processes.

Thermal conductivity due to electron-ion collisions in the solid phase $\kappa_{\rm ei}^{\rm s}$ can be written as [27]

$$\kappa_{\rm ei}^{\rm s} = \frac{1}{3} C_v v \lambda_{\rm s} = \frac{1}{3} n k_{\rm B} U(t) v_{\rm F} \lambda_{\rm s}. \tag{2}$$

Here we introduced the dimensionless temperature $t = 6k_{\rm B}T_{\rm e}/\varepsilon_{\rm F} = 6k_{\rm B}T_{\rm e}/(\varepsilon_{\rm F0}x^{2/3})$; $x = \rho/\rho_0$ is the ratio of current density ρ and density $\rho_0 = 9.019$ g/cm^3 at zero temperature and zero pressure. In the product of the s-electron heat capacity of a unit volume (its calculation in a two-parabolic model of the electronic spectrum on the example of gold is described in the work [19])

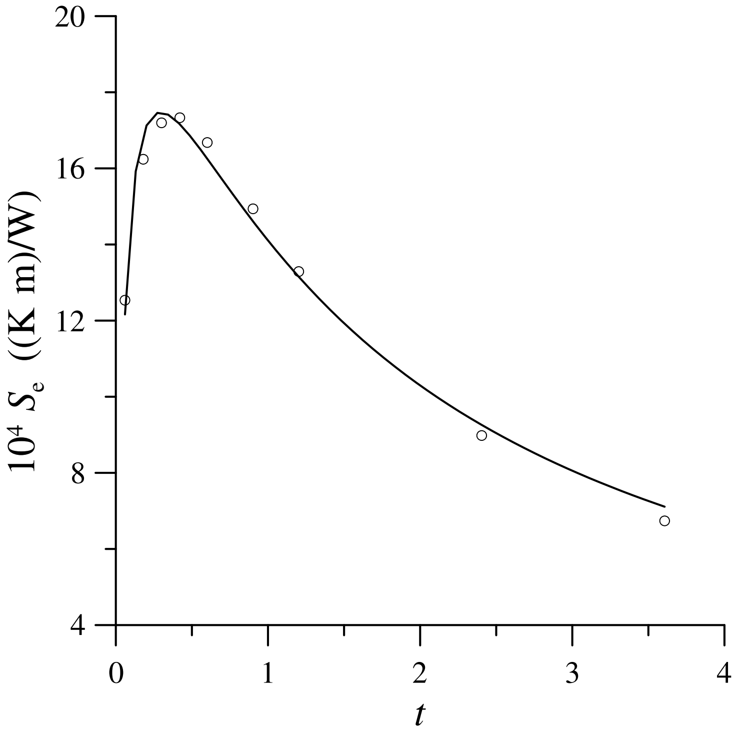

Figure 2. Thermal resistance of nickel due to the electron–electron scattering at the reduced density $x = 1$ as a function of the reduced electron temperature t. Circles are the results of calculation made as in [16], full line is the calculation by formula (15).

and the average velocity of s-electrons $v = v_{\mathrm{F}}\sqrt{1 + 3k_{\mathrm{B}}T_{\mathrm{e}}/(2\varepsilon_{\mathrm{F}})}$ we highlighted dependent on t dimensionless factor $U(t)$. The function $U(t)$ was calculated at $x = 1$ and can be approximated by the expression

$$U(t) = \frac{t(1 + c_1 t^2)}{1 + c_2 t^{c_3}} \tag{3}$$

with $c_1 = 5.269$, $c_2 = 3.059$, $c_3 = 2.094$. In addition, we designated ε_{F} and $\varepsilon_{\mathrm{F0}}$ the Fermi energy at the current density and density with $x = 1$ respectively. Fermi velocity $v_{\mathrm{F}} = p_{\mathrm{F}}/m^*$ depends on the concentration of atoms n at a constant number of conduction electrons per atom through the Fermi momentum $p_{\mathrm{F}} \propto n^{1/3}$. Considering the effective mass m^* independent on density, we have $v_{\mathrm{F}} = v_{\mathrm{F0}} x^{1/3}$, where v_{F0} is the Fermi velocity at the reduced density x=1.

The mean free path of s-electrons during scattering by phonons in the solid phase $\lambda_{\mathrm{s}} = 1/(n\Sigma)$. In this case, the scattering cross section

$$\Sigma \propto u_0^2 \frac{T_{\mathrm{i}}}{\theta}, \tag{4}$$

where $u_0^2 \propto \hbar^2/(M k_{\mathrm{B}} \theta)$ is the squared amplitude of the zero-point vibrations of atoms of mass M, and θ is the Debye temperature [27]. So for λ_{s} we obtain

$$\lambda_{\mathrm{s}} \propto \left(n \frac{T_{\mathrm{i}}}{\theta} \frac{\hbar^2}{M k_{\mathrm{B}} \theta} \right)^{-1} \propto \frac{M k_{\mathrm{B}}}{\hbar^2 T_{\mathrm{i}}} \frac{\theta^2}{n} \propto \frac{\theta^2}{n T_{\mathrm{i}}}. \tag{5}$$

To find the dependence of the Debye temperature on density, we use the curve of the dependence of cold pressure on density (concentration of atoms) $p_{\mathrm{c}}(n)$ from [25, 26, 28–30]. This curve

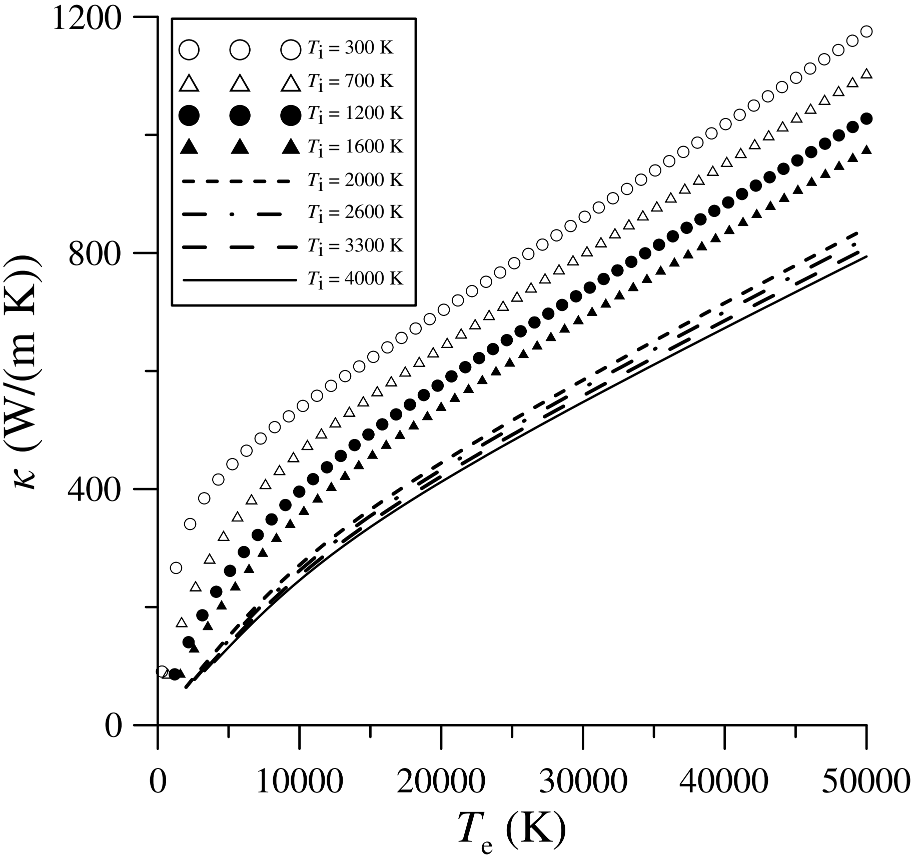

Figure 3. Electron thermal conductivity of nickel of normal density as a function of the electron temperature at several values of the temperature of ions.

describes well the experimental data. In [25] it is given by the equation of state in the Birch–Murnaghan form of the dependence of pressure on the reduced density x introduced above:

$$p_c(x) = \frac{3}{2}\beta_0(x^{7/3} - x^{5/3})\left[1 + \frac{3}{4}(x^{2/3} - 1)(\beta_1 - 4)\right] \tag{6}$$

with the parameters $\beta_0 = 189.0$ GPa, $\beta_1 = 4.70$. The dependence of cold pressure on the reduced density can be well approximated as the sum of two terms with power-law dependencies on the reduced density, one of which corresponds to repulsion, and the other to the attraction of atoms:

$$p_c = p_{c0}\, x\, (x^a - x^b). \tag{7}$$

From comparison with [25] we find $a = 2.0196, b = 0.6806, p_{c0} = 141.1384$ GPa. Comparison of the two-term approximation of cold pressure (7), as well as calculated by the Birch–Murnaghan formula from [25] and data from [26] is shown in figure 1.

With adopted two-term formula (7) for cold pressure, the expression for the squared Debye temperature has the form

$$\theta^2(x) = \left(\frac{\hbar}{k_B} c_s k_D\right)^2 x^{2/3} \frac{(a+1)x^a - (b+1)x^b}{a-b}. \tag{8}$$

In this expression, the direction-averaged sound velocity c_s and Debye wave number k_D are taken at equilibrium density ($x = 1$). Function

$$y(x) = \frac{(a+1)x^a - (b+1)x^b}{a-b} \tag{9}$$

in (8) becomes negative with decreasing density. To avoid this circumstance, we represent the Debye temperature in the form of an expression close to (8), but without features for small x, so

$$\theta^2(x) = \theta^2(1)x^{2/3}\bar{y}(x), \tag{10}$$

where

$$\bar{y}(x) = \frac{(1+c_{\mathrm{ab}})x^{\alpha}}{1+c_{\mathrm{ab}}x^{\beta}}, \qquad \alpha = 2a+1, \qquad \beta = a+1, \qquad c_{\mathrm{ab}} = \frac{a-b}{b+1}. \tag{11}$$

Functions $y(x)$ (9) and $\bar{y}(x)$ in (11) together with their derivatives have the same values at $x = 1$ and the same asymptotics at large x. With the use of function $\bar{y}(x)$ we have $\lambda_{\mathrm{si}} \propto \bar{y}(x)/(T_{\mathrm{i}}x^{1/3})$. Therefore, we obtain

$$\kappa^{\mathrm{s}}_{\mathrm{ei}}(T_{\mathrm{e}}, T_{\mathrm{i}}, x) \propto U(t)xx^{1/3}\frac{\bar{y}(x)}{T_{\mathrm{i}}x^{1/3}} \propto U(t)\frac{x\bar{y}(x)}{T_{\mathrm{i}}}. \tag{12}$$

We denote $x_r = 8.909/9.019$ the reduced density of nickel at room temperature $T_r = 300$ K and normal pressure. To satisfy the condition that the experimental value of the thermal conductivity in this case is 90.8 W/(m K), we take the thermal conductivity in W/(m K) at the scattering of electrons by ions in the solid phase as

$$\kappa^{\mathrm{s}}_{\mathrm{ei}}(T_{\mathrm{e}}, T_{\mathrm{i}}, x) = 96\frac{x}{x_{\mathrm{r}}}\frac{\bar{y}(x)}{\bar{y}(x_{\mathrm{r}})}\frac{T_{\mathrm{r}}}{T_{\mathrm{i}}}\frac{U(t)}{U(t_{\mathrm{r}})}. \tag{13}$$

Here $t_{\mathrm{r}} = 6k_{\mathrm{B}}T_{\mathrm{r}}/(\varepsilon_{\mathrm{F0}}{x_{\mathrm{r}}}^{2/3})$. Difference between 90.8 and 96 W/(m K) values arises when taking into account electron–electron scattering.

The thermal conductivity at electron–electron scattering (in the case of nickel, it is s–s and s–d scattering) was calculated similarly to how it was done in relaxation time approximation in [16, 18]. In electron–electron scattering, scattering of s-electrons by s-electrons can be distinguished (with a frequency ν_{ss}) and their scattering by d-electrons (with a frequency of ν_{sd}). This gives for thermal resistance in electron–electron scattering

$$S_{\mathrm{e}}(T_{\mathrm{e}}, x) = \frac{1}{\kappa_{\mathrm{ee}}} = \frac{1}{\kappa_{\mathrm{ss}}} + \frac{1}{\kappa_{\mathrm{sd}}}. \tag{14}$$

Thermal resistance was calculated for different values of electron temperature T_{e} up to 60 kK, not exceeding the Fermi temperature at $x = 1$. So we restrict our consideration by this interval of the temperatures of electrons. The results of these calculations of thermal resistance due to the electron–electron scattering are shown in figure 2 as well as their approximation by the expression

$$S_{\mathrm{e}}(T_{\mathrm{e}}, x) = \frac{s_1 t}{x(1 + s_2 t + s_3 t^2)} \tag{15}$$

with $s_1 = 0.0421, s_2 = 17.321, s_3 = 11.550$, which gives the value of S_{e} in $[\mathrm{W/(m\,K)}]^{-1}$. As a result, for the inverse thermal conductivity in the solid phase, we have

$$\frac{1}{\kappa_{\mathrm{s}}(T_{\mathrm{e}}, T_{\mathrm{i}}, x)} = S_{\mathrm{e}}(T_{\mathrm{e}}, x) + \frac{1}{\kappa^{\mathrm{s}}_{\mathrm{ei}}(T_{\mathrm{e}}, T_{\mathrm{i}}, x)}. \tag{16}$$

We suppose the expression for the thermal resistance S_{e} due to electron–electron scattering has the same form in both the solid and liquid phases.

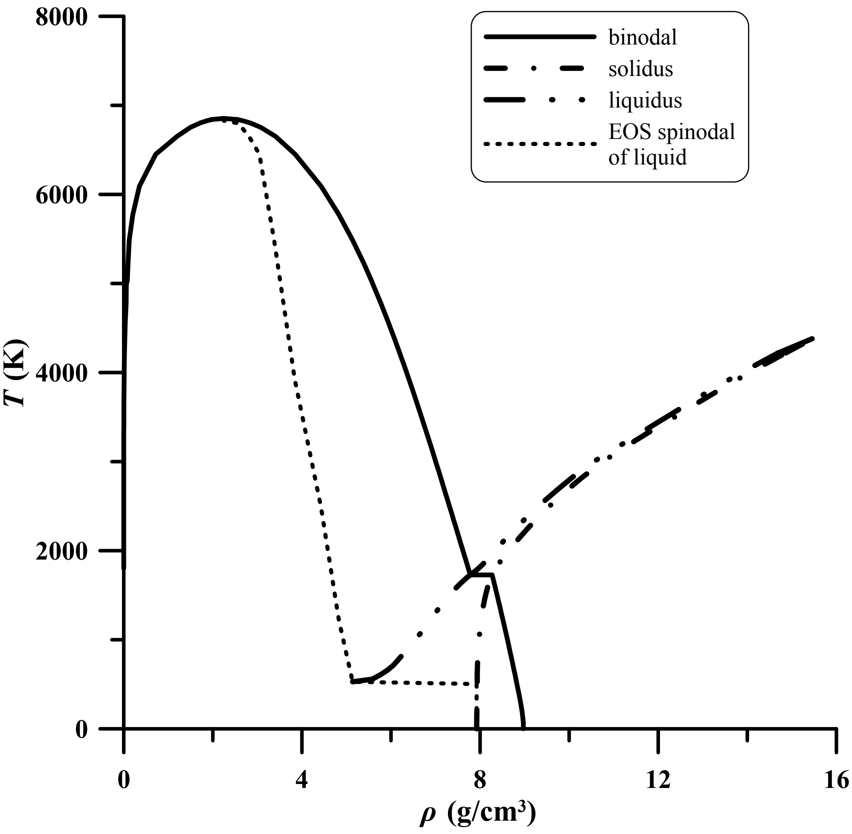

Figure 4. Phase diagram of nickel used to calculate its isochoric thermal conductivity.

3. Electron thermal conductivity of nickel in the liquid phase

We calculate the thermal conductivity of the melt of two-temperature nickel. The electron–electron contribution is still given by formula (14) for thermal resistance. It is required to write an approximation expression for the contribution of electron–ion scattering. We assume that in the liquid phase the mean free path of electrons in electron–ion scattering $\lambda_{\rm l}$ can be written in factorized form as $\lambda_{\rm l} = {n_0}^{-1/3} W(T_{\rm i}) x^{-1/3}$ and again using the value $U(t)$, we have for the coefficient of thermal conductivity due to electron–ion scattering

$$\kappa^{\rm l}_{\rm ei}(T_{\rm e}, T_{\rm i}, x) \propto U(t) x x^{1/3} W(T_{\rm i}) x^{-1/3} \propto U(t) x W(T_{\rm i}). \tag{17}$$

The function $W(T_{\rm i})$ is chosen in the form

$$W(T_{\rm i}) = \frac{1 + T_1/T_{\rm i}}{1 + T_2/T_{\rm i}} \tag{18}$$

with $T_1 = 7650$ K, $T_2 = 2580$ K, similar to how it was done for liquid aluminum based on calculations made in the Ziman approximation [31,32]. Then we obtain thermal conductivity in the liquid phase due to electron–ion scattering in the form

$$\kappa^{\rm l}_{\rm ei}(T_{\rm e}, T_{\rm i}, x) = 61 \frac{x}{x_{\rm lm}} \frac{U(t)}{U(t_{\rm lm})} \frac{W(T_{\rm i})}{W(T_{\rm m})}. \tag{19}$$

Here we introduced the reduced density of the liquid phase at the melting point under normal pressure (i.e., at $T_{\rm m} = 1728$ K, $\rho_{\rm lm} = 7.81$ g/cm^3) $x_{\rm lm} = \rho_{\rm lm}/\rho_0$ and $t_{\rm lm} = 6k_{\rm B}T_{\rm m}/(\varepsilon_{\rm F0}{x_{\rm lm}}^{2/3})$, and also took into account the value of the thermal coefficient in the liquid phase at the melting point equal to 55 W/(m K) [33–35] (again difference between 61 and 55 W/(m K) is due to the

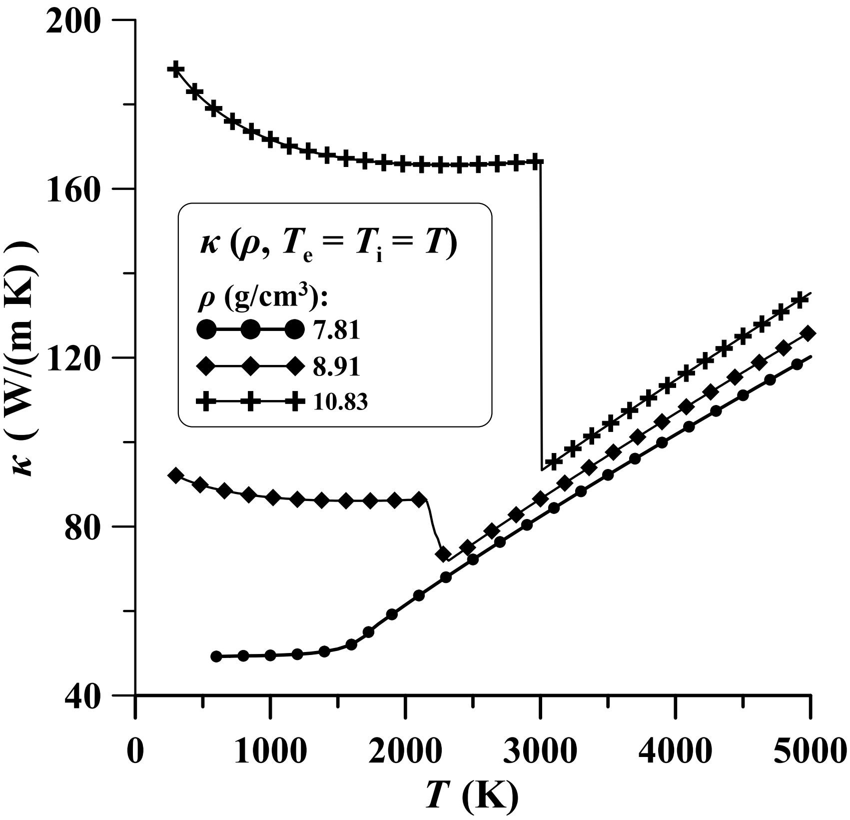

Figure 5. Electron thermal conductivity of nickel in dependence on temperature, equal for electrons and ions, for different values of density with taking into account phase transition.

electron–electron scattering). The total thermal conductivity in the liquid phase is found taking into account $\kappa_{\rm ee}$, so for thermal resistance we have

$$\frac{1}{\kappa_{\rm l}(T_{\rm e},T_{\rm i},x)}=S_{\rm e}(T_{\rm e},x)+\frac{1}{\kappa_{\rm ei}^{\rm l}(T_{\rm e},T_{\rm i},x)}. \tag{20}$$

Electron thermal conductivity of nickel in dependence on the electron temperature at different ion temperatures at normal density is sown in figure 3.

To show the influence of the phase transition in the dependence of thermal conductivity on the temperature we used the phase diagram of nickel, calculated by K V Khishchenko in the framework of model developed in [36–38] and presented in figure 4. In figure 5 isochoric electron thermal conductivity of nickel is exhibited as a function of temperature, equal both for ions and electrons. Here three values of density and different phase states (solid and liquid) are presented.

4. Electron thermal conductivity of aluminum

The parameters of the two-term representation of cold pressure in Al are $p_{\rm c0} = 250.896$ GPa, $a = 1.2693$, $b = 0.9425$.

Acting for aluminum, as well as for nickel, taking into account only one s, p-band of electrons, we obtain thermal resistance due to electron–electron scattering in the form

$$S_{\rm e}(T_{\rm e},x)=\frac{s_1 t}{x(1-s_2 t^{1/2}+s_3 t+s_4 t^2)} \tag{21}$$

with $s_1 = 0.000\,4771$, $s_2 = 0.5096$, $s_3 = 0.5307$, $s_4 = 0.064\,41$. Here in $t = 6k_{\rm B}T_{\rm e}/(\varepsilon_{\rm F0}x^{2/3})$ for aluminum, $\varepsilon_{\rm F0} = 11.1$ eV, and $x = \rho/\rho_0$ with $\rho_0 = 2.75$ g/cm^3.

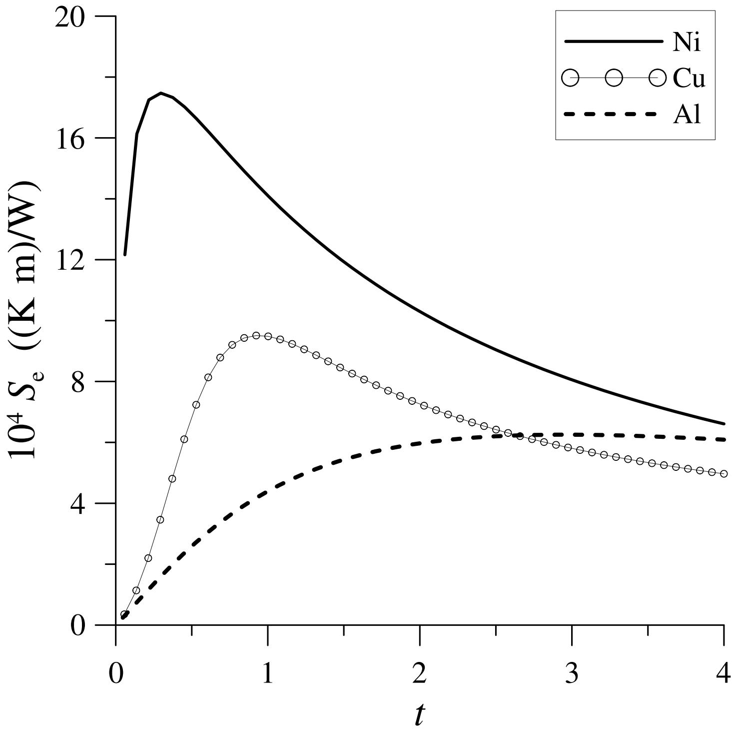

Figure 6. Thermal resistance due to the electron–electron scattering at the reduced density $x = 1$ for Ni (solid line), Cu (circles) and Al (dashed line) in dependence on the reduced electron temperature t.

In figure 6 we presented the thermal resistance due to the electron–electron scattering at the reduced density $x = 1$ of aluminum together with its value for nickel from formula (15) and copper taken from [16].

The function $U(t)$ in the solid phase of aluminum can be written as

$$U(t) = \frac{t(1 + c_{\rm s1} t^2)}{1 + c_{\rm s2} t^{c_{\rm s3}}} \tag{22}$$

with $c_{\rm s1} = 0.3453$, $c_{\rm s2} = 0.3685$, $c_{\rm s3} = 2.4089$. The thermal conductivity of solid aluminum due to electron–ion scattering can be represented as

$$\kappa_{\rm ei}^{\rm s}(T_{\rm e}, T_{\rm i}, x) = k_{\rm is} \frac{x}{x_{\rm r}} \frac{\bar{y}(x)}{\bar{y}(x_{\rm r})} \frac{T_{\rm r}}{T_{\rm i}} \frac{U(t)}{U(t_{\rm r})}. \tag{23}$$

Here $t_r = 6k_{\rm B}T_{\rm r}/(\varepsilon_{\rm F0} {x_{\rm r}}^{2/3})$ with $x_{\rm r} = 2.70/2.75$.

Then, as for nickel, in the solid phase

$$\frac{1}{\kappa_{\rm s}(T_{\rm e}, T_{\rm i}, x)} = S_{\rm e}(T_{\rm e}, x) + \frac{1}{\kappa_{\rm ei}^{\rm s}(T_{\rm e}, T_{\rm i}, x)}. \tag{24}$$

Coefficient $k_{\rm is}$ in (23) is taken equal to 237.5 W/(m K) to give the thermal conductivity value for aluminum at normal conditions from (24) with taking into account electron–electron scattering $\kappa_{\rm s} = 237$ W/(m K).

In the liquid phase of aluminum, the thermal conductivity due to electron–ion scattering can be approximated by the expression

$$\kappa_{\rm ei}^{\rm l}(T_{\rm e}, T_{\rm i}, x) = k_{\rm il} \frac{x}{x_{\rm lm}} \frac{U_{\rm l}(t)}{U_{\rm l}(t_{\rm lm})} \frac{W(T_{\rm i})}{W(T_{\rm m})} \tag{25}$$

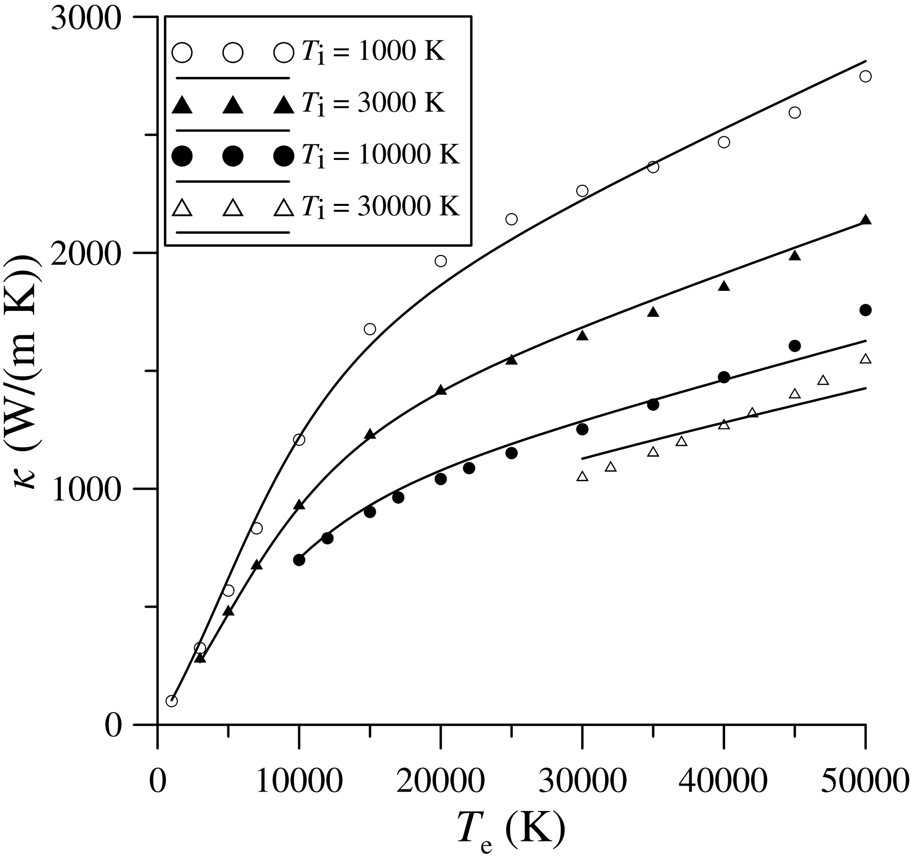

Figure 7. Electron thermal conductivity of liquid aluminum due to the electron–ion scattering in dependence on the electron temperature T_e at different temperatures of ions. Aluminum density is 2.35 g/cm^3. Symbols are results of calculations made in Ziman approach (in [32]), full lines show thermal conductivity obtained by the use of approximation (25).

with $x_\mathrm{lm} = 2.35/2.75$, $t_\mathrm{lm} = 6k_\mathrm{B}T_\mathrm{m}/(\varepsilon_\mathrm{F0}x_\mathrm{lm}{}^{2/3})$ and a melting temperature $T_\mathrm{m} = 933.6$ K. The functions included here are

$$U_\mathrm{l}(t) = \frac{t(1 + c_\mathrm{l1}t + c_\mathrm{l2}t^2)}{1 + c_\mathrm{l3}t^{c_\mathrm{l4}}}, \tag{26}$$

$$W(T_\mathrm{i}) = \frac{1 + T_1/T_\mathrm{i}}{1 + T_2/T_\mathrm{i}} \tag{27}$$

with $c_\mathrm{l1} = 1.5443$, $c_\mathrm{l2} = 1.3767$, $c_\mathrm{l3} = 2.9959$, $c_\mathrm{l4} = 2.1633$ and $T_1 = 4130$ K, $T_2 = 1390$ K. And taking into account the electron–electron scattering for the inverse coefficient of electronic thermal conductivity of aluminum in the liquid phase, we have

$$\frac{1}{\kappa_\mathrm{l}(T_\mathrm{e}, T_\mathrm{i}, x)} = S_\mathrm{e}(T_\mathrm{e}, x) + \frac{1}{\kappa_\mathrm{ei}^\mathrm{l}(T_\mathrm{e}, T_\mathrm{i}, x)}. \tag{28}$$

We take coefficient k_il in (25) to be $k_\mathrm{il} = 98.3$ W/(m K) in order to obtain the value of the thermal conductivity at the melting point T_m at normal pressure from (28) $\kappa_\mathrm{l} = 98$ W/(m K).

The thermal conductivity due to electron–ion scattering, calculated in the Ziman approach and by formula (25), is shown in figure 7 depending on electron temperature for four values of ion temperature $T_\mathrm{i} = 1000$, 3000, 10 000, 30 000 K and density 2.35 g/cm^3. Up to the temperature of ions $T_\mathrm{i} = 30$ kK, the use of the expression (25) for the calculation of the thermal conductivity

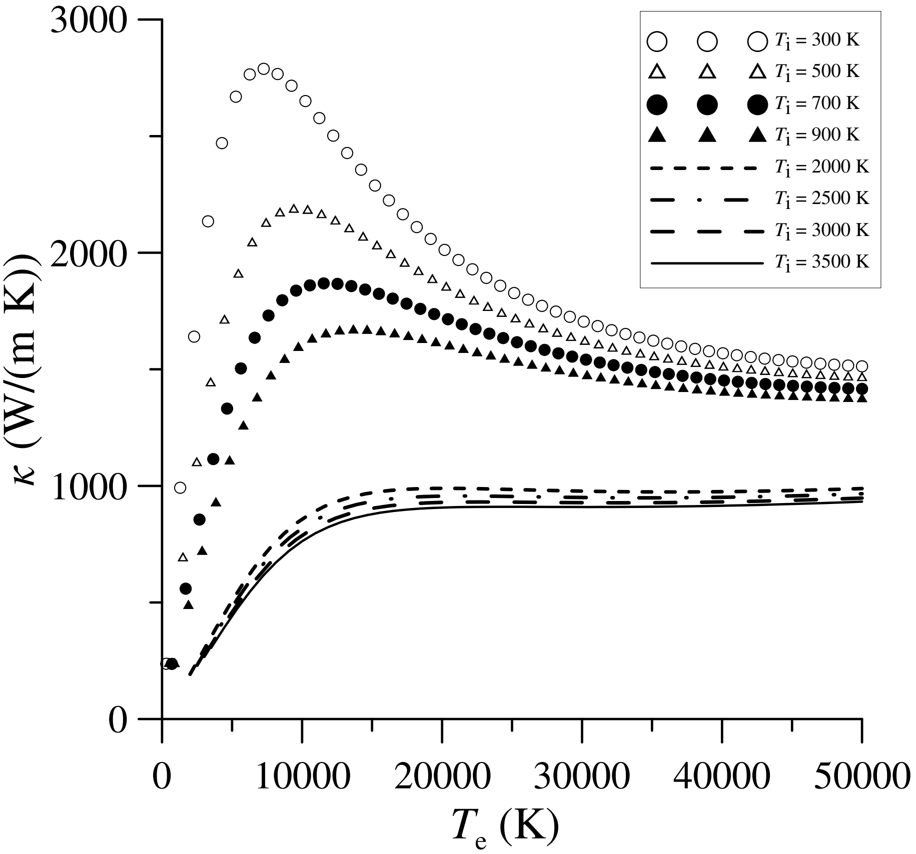

Figure 8. Electron thermal conductivity of aluminum of normal density in dependence on the electron temperature at several ion temperatures.

due to the electron–ion scattering gives results that are in good agreement with those obtained by applying the Ziman approximation. The ion temperature range for the applicability of expression (25) up to 30 kK covers the range of ion temperatures that we consider when studying the ablation of multilayer aluminum and nickel targets.

Thermal conductivity of aluminum is presented in figure 8 as a function of the temperature of electrons for several ion temperatures at normal density.

5. Conclusion

We have presented analytical expressions approximating thermal conductivity of nickel and aluminum, those metals, which are used particularly in experiments on the ablation of multilayer targets. Expressions obtained give thermal conductivity of these materials in dependence of electron and ion temperatures and density and take into account their phase state (solid or liquid). These expressions for electron thermal conductivity can be applied in the hydrodynamic codes used when studying ablation processes in these metals.

Acknowledgments

Authors wish to thank K V Khishchenko for supplying the phase diagram of nickel.

One of the authors (NAI) acknowledges support from the Russian Science Foundation (grant No. 19-19-00697).

References

[1] Rethfeld B, Ivanov D S, Garcia M E and Anisimov S I 2017 *J. Phys. D* **50** 193001
[2] Inogamov N A *et al* 2015 *Eng. Fail. Anal.* **47** 328–37
[3] Inogamov N A, Zhakhovsky V V, Khokhlov V A, Petrov Y V and Migdal K P 2016 *Nanoscale Res. Lett.* **11** 177
[4] Bulgakova N M and Zhukov V P 2014 Continuum models of ultrashort laser-matter interaction in application to wide-bandgap dielectrics *Lasers in Materials Science* ed Castillejo M *et al* (Heidelberg: Springer) pp 101–23
[5] Inogamov N A *et al* 2011 *Contrib. Plasma Phys.* **51** 419–26
[6] Ding P J, Liu Q C, Lu X, Liu X L, Sun S H, Liu Z Y, Hu B T and Li Y H 2012 *Nucl. Instrum. Methods Phys. Res., B* **286** 40–4
[7] Inogamov N A *et al* 2011 *Contrib. Plasma Phys.* **51** 361–6
[8] Ohkubo T, Kuwata M, Lukyanchuk B and Yabe T 2003 *Appl. Phys.* A **77** 271
[9] Povarnitsyn M E, Itina T E, Levashov P R and Khishchenko K V 2007 *Appl. Surf. Sci.* **253** 6343–6
[10] Povarnitsyn M E, Itina T E, Sentis M, Levashov P R and Khishchenko K V 2007 *Phys. Rev.* B **75** 235414
[11] Povarnitsyn M E, Itina T E, Levashov P R and Khishchenko K V 2011 *Appl. Surf. Sci.* **257** 5168–71
[12] Povarnitsyn M E, Itina T E, Levashov P R and Khishchenko K V 2013 *Phys. Chem. Chem. Phys.* **15** 3108
[13] Povarnitsyn M E and Itina T E 2014 *Appl. Phys.* A **117** 175–8
[14] Migdal K P, Petrov Y V, Il'nitsky D K, Zhakhovsky V V, Inogamov N A, Khishchenko K V, Knyazev D V and Levashov P R 2016 *Appl. Phys. A* **122** 408
[15] Petrov Y V, Migdal K P, Knyazev D V, Inogamov N A and Levashov P R 2016 *J. Phys.: Conf. Ser.* **774** 012103
[16] Petrov Y V, Migdal K P, Inogamov N A and Anisimov S I 2016 *JETP Lett.* **104** 431
[17] Migdal K P, Zhakhovsky V V, Yanilkin A V, Petrov Yu V and Inogamov N A 2019 *Appl. Surf. Sci* **478** 818–30
[18] Petrov Y V, Inogamov N A and Migdal K P 2013 *JETP Lett.* **97** 20–7
[19] Petrov Yu V, Inogamov N A, Anisimov S I, Migdal K P, Khokhlov V A and Khishchenko K V 2015 *J. Phys.: Conf. Ser.* **653** 012087
[20] Migdal K P, Il'nitsky D K, Petrov Yu V and Inogamov N A 2015 *J. Phys.: Conf. Ser.* **653** 012086
[21] Ashitkov S I *et al* 2016 *J. Phys.: Conf. Ser.* **774** 012097
[22] Petrov Y V, Khokhlov V A, Inogamov N A, Khishchenko K V and Anisimov S I 2016 *J. Phys.: Conf. Ser.* **774** 012099
[23] Migdal K P, Petrov Y V and Inogamov N A 2013 *Proc. SPIE* **9065** 906503
[24] Animalu A O E 1977 *Intermediate Quantum Theory of Crystalline Solids* (Englewood Cliffs, NJ: Prentice-Hall)
[25] Kerley G I 2003 Equations of state for Be, Ni, W and Au *Report* SAND 2003-3784 (Albuquerque, NM: Sandia National Laboratories)
[26] Lomonosov I V and Gryaznov V K 2016 *Contrib. Plasma Phys.* **56** 302–7
[27] Ziman J M 1972 *Principles of the Theory of Solids* (Cambridge, GB: Cambridge University Press)
[28] Bushman A V and Fortov V E 1983 *Sov. Phys. Usp.* **26** 465–96
[29] Bushman A V, Lomonosov I V and Fortov V E 1993 *Sov. Tech. Rev. B* **5** 1
[30] Levashov P R and Khishchenko K V 2007 *AIP Conf. Proc.* **955** 59–62
[31] Petrov Yu V, Inogamov N A, Mokshin A V and Galimzyanov B N 2018 *J. Phys.: Conf. Ser.* **946** 012096
[32] Petrov Yu V, Inogamov N A, Migdal K P, Mokshin A V and Galimzyanov B N 2019 *J. Phys.: Conf. Ser.* **1147** 012069
[33] Nagata K, Fukuyama H, Taguchi K, Ishii H and Hayashi M 2003 *High Temp. Mater. Processes* **22** 267–73
[34] Nishi T, Shibata H, Waseda Y and Ohta H 2003 *Metall. Mater. Trans.* A **34** 2801–7
[35] Zinovyev V Y, Polev V F, Taluts S G, Zinovyeva G P and Ilinykh S A 1986 *Phys. Met. Metallogr.* **61** 85–92
[36] Khishchenko K V 2008 *J. Phys.: Conf. Ser.* **121** 022025
[37] Khishchenko K V 2008 *J. Phys.: Conf. Ser.* **98** 032023
[38] Khishchenko K V 2015 *J. Phys.: Conf. Ser.* **653** 012081